

Photon Structure Functions: past, present, future

T. Ueda¹, T. Uematsu² and K. Sasaki³

1. Nikhef Theory Group, Science Park 105, 1098 XG Amsterdam, The Netherlands

2. Institute for Liberal Arts and Sciences, Kyoto University, Kyoto 606-8501, Japan

3. Faculty of Engineering, Yokohama National University, Yokohama 240-8501, Japan

Abstract

We review the photon structure functions in the past and at present and discuss the future of this field.

Keywords

Photon structure functions; parton distributions in the photon.

1 Prologue

In e^+e^- collider experiments, the two-photon process in which one of the virtual photons is very far off shell (large $Q^2 \equiv -q^2$) while the other is close to the mass shell (small $P^2 \equiv -p^2$) can be viewed as a deep-inelastic electron-photon scattering [1]. In the deep-inelastic scattering off a photon target, we can study the structure of photon. Two (unpolarized) structure functions $F_2^\gamma(x, Q^2)$ and $F_L^\gamma(x, Q^2)$ of the real photon ($P^2 = 0$) can be measured in the single-tag events, while in the double-tag events we observe $F_2^\gamma(x, Q^2, P^2)$ and $F_L^\gamma(x, Q^2, P^2)$ of the virtual photon.

2 Photon structure functions — Past

The structure functions $F_2^\gamma(x, Q^2)$ and $F_L^\gamma(x, Q^2)$ were first studied in the parton model [2] and then investigated in perturbative QCD (pQCD). The leading order (LO) [3] and the next-to-leading order (NLO) [4] QCD contributions to F_2^γ were calculated and the moments of F_2^γ is expressed as

$$\int_0^1 dx x^{n-2} F_2^\gamma(x, Q^2) = \frac{\alpha}{4\pi} \frac{1}{2\beta_0} \left\{ \frac{4\pi}{\alpha_s(Q^2)} a_n + b_n + h_n(\alpha_s(Q^2)) + \mathcal{O}(\alpha_s(Q^2)) \right\} \quad (1)$$

where x is the Bjorken variable, β_0 is the one-loop QCD β function and α ($\alpha_s(Q^2)$) is the QED (QCD running) coupling constant. Since $1/\alpha_s(Q^2)$ behaves as $\ln(Q^2/\Lambda^2)$ at large Q^2 , where Λ is the QCD scale parameter, the first term $a_n/\alpha_s(Q^2)$ dominates over the b_n term and also over the hadronic term $h_n(\alpha_s(Q^2))$. The LO contributions a_n were definite [3]. Meanwhile, the NLO corrections b_n were calculated only for $n > 2$ [4]. For $n > 2$, the hadronic moments $h_n(\alpha_s(Q^2))$ vanish in the large- Q^2 limit and the b_n terms give finite contributions. However, at $n = 2$, the hadronic energy-momentum tensor operator comes into play. Due to the conservation of this operator, b_n shows a singularity at $n = 2$ and $h_{n=2}(\alpha_s(Q^2))$ does not vanish at large Q^2 . Actually, $h_n(\alpha_s(Q^2))$ also develops a singularity at $n = 2$ which cancels out the one of b_n , and $h_n(\alpha_s(Q^2))$ and b_n in combination give a finite but perturbatively incalculable contribution at $n = 2$ [5]. The fact that a definite information on the NLO second moment is missing prevents us to fully predict the shape and magnitude of the structure function of $F_2^\gamma(x, Q^2)$ up to the order $\mathcal{O}(\alpha)$.

It was then pointed out [5] that the situation changes significantly when we analyze the structure function of a virtual photon with P^2 much larger than Λ^2 , more specifically, in the kinematical region $\Lambda^2 \ll P^2 \ll Q^2$. In this region, the hadronic component of the photon can also be dealt with *perturbatively* and thus a definite prediction of the whole structure function, its shape and magnitude, may become possible. In fact, the virtual photon structure function $F_2^\gamma(x, Q^2, P^2)$ for $\Lambda^2 \ll P^2 \ll Q^2$ was calculated in LO (the order α/α_s) and NLO (the order α) [5] without any unknown parameters. It is

notable that the pathology of singularity, which appeared at $n = 2$ in the term b_n of Eq. (1) for the real photon target, disappeared from the moments of $F_2^\gamma(x, Q^2, P^2)$.

Then what happens to the moments of $F_2^\gamma(x, Q^2, P^2)$ with arbitrary P^2 but $P^2 \ll Q^2$? If we employ the framework of the operator product expansion supplemented by the renormalization group method, we need to know the photon matrix element (PME), $\langle \gamma(p) | O_n^i(\mu^2) | \gamma(p) \rangle$, with $i = S, G, NS, \gamma$, where $|\gamma(p)\rangle$ is the ‘‘target’’ virtual photon state with momentum p , O_n^i are the relevant twist-2 spin- n operators and μ^2 is the renormalization point. The indices S, G, NS and γ refer to singlet quark, gluon, nonsinglet quark and photon, respectively. To lowest order in the QED coupling, $\langle \gamma(p) | O_n^\gamma(\mu^2) | \gamma(p) \rangle = 1$. Choosing the renormalization point at $\mu^2 = Q_0^2$ with the condition $\Lambda^2 \ll Q_0^2 \ll Q^2$, we write the PME’s of the hadronic operators $\vec{O}_n = (O_n^S, O_n^G, O_n^{NS})$ as $\langle \gamma(p) | \vec{O}_n(\mu) | \gamma(p) \rangle|_{\mu^2=Q_0^2} = \frac{\alpha}{4\pi} \vec{A}_n(Q_0^2; P^2)$. Now when photon state becomes far off-shell and P^2 approaches Q_0^2 , its point-like nature prevails and $\vec{A}_n(Q_0^2; P^2)$ becomes calculable perturbatively. Let us put $\vec{A}_n(Q_0^2; P^2 = Q_0^2) \equiv \vec{A}_n^{(1)}$ in one-loop order. For an arbitrary P^2 in the range $0 \leq P^2 \leq Q_0^2$, we divide $\vec{A}_n(Q_0^2; P^2)$ into two pieces such that $\vec{A}_n(Q_0^2; P^2) = \vec{\tilde{A}}_n(Q_0^2; P^2) + \vec{A}_n^{(1)}$. Note that $\vec{\tilde{A}}_n(Q_0^2; P^2)$ contains nonperturbative contributions (i.e., hadronic components) when P^2 is in the range $0 \leq P^2 \leq Q_0^2$, and satisfies the boundary condition by definition $\vec{\tilde{A}}_n(Q_0^2; P^2 = Q_0^2) = 0$. Then the following formula is obtained for the moments of F_2^γ up to NLO in QCD (the extension to NNLO is straightforward),

$$\begin{aligned} \int_0^1 dx x^{n-2} F_2^\gamma(x, Q^2, P^2) / \left(\frac{\alpha}{4\pi} \frac{1}{2\beta_0} \right) &= \frac{4\pi}{\alpha_s(Q^2)} \sum_{i=+,-,NS} \frac{\tilde{\mathcal{L}}_i^n}{1+d_i^n} \left\{ 1 - \left(\frac{\alpha_s(Q^2)}{\alpha_s(Q_0^2)} \right)^{1+d_i^n} \right\} \\ &+ \sum_{i=+,-,NS} \frac{\tilde{\mathcal{A}}_i^n}{d_i^n} \left\{ 1 - \left(\frac{\alpha_s(Q^2)}{\alpha_s(Q_0^2)} \right)^{d_i^n} \right\} + \sum_{i=+,-,NS} \frac{\tilde{\mathcal{B}}_i^n}{1+d_i^n} \left\{ 1 - \left(\frac{\alpha_s(Q^2)}{\alpha_s(Q_0^2)} \right)^{1+d_i^n} \right\} + \mathcal{C}^n \\ &+ 2\beta_0 \vec{\tilde{A}}_n(Q_0^2; P^2) \cdot \sum_{i=+,-,NS} P_i^n \vec{C}_n(1, 0) \left(\frac{\alpha_s(Q^2)}{\alpha_s(Q_0^2)} \right)^{d_i^n}, \end{aligned} \quad (2)$$

which is applicable for an arbitrary target mass squared P^2 in the range $0 \leq P^2 \leq Q_0^2$. Here the coefficients $\tilde{\mathcal{L}}_i^n$, $\tilde{\mathcal{A}}_i^n$, $\tilde{\mathcal{B}}_i^n$ and \mathcal{C}^n are written in terms of the quantities calculable by the pQCD. Their explicit expressions are found in Ref. [5]. The exponents d_i^n are given by $d_i^n = \lambda_i^n / 2\beta_0$ ($i = +, -, NS$) where λ_i^n are the eigenvalues of the one-loop anomalous dimension matrix $\hat{\gamma}_n^{(0)}$, which is expanded as $\hat{\gamma}_n^{(0)} = \sum_i \lambda_i^n P_i^n$ with P_i^n being the projection operators [4]. The terms a_n and b_n in Eq. (1) correspond to $\sum_i \tilde{\mathcal{L}}_i^n / (1+d_i^n)$ and $\sum_i \tilde{\mathcal{A}}_i^n / d_i^n + \sum_i \tilde{\mathcal{B}}_i^n / (1+d_i^n) + \mathcal{C}^n$, respectively. Since $d_{-}^{n=2} = 0$, $\tilde{\mathcal{A}}_i^n / d_i^n$ and thus b_n become singular at $n = 2$. But we see that the product $(\tilde{\mathcal{A}}_i^n / d_i^n) \times \left[1 - (\alpha_s(Q^2) / \alpha_s(Q_0^2))^{d_i^n} \right]$ is finite in the limit $n \rightarrow 2$. There appear no singularities in the expression in Eq. (2). When P^2 approaches Q_0^2 , the last term with $\vec{\tilde{A}}_n(Q_0^2; P^2)$ vanishes, and we recover the result of Ref. [5]. For an arbitrary P^2 below Q_0^2 , however, we need to use the experimental data once or resort to some nonperturbative methods (like lattice QCD) or employ models (like the vector meson dominance model) to estimate $\vec{\tilde{A}}_n(Q_0^2; P^2)$.

3 Photon structure functions — Present

The work toward the next-to-next-to-leading order (NNLO) ($\mathcal{O}(\alpha\alpha_s)$) analysis of the real photon F_2^γ started in Ref. [6], where the lowest six even-integer Mellin moments of the three-loop photon-parton (quark and gluon) splitting functions were calculated and the parton distributions in the real photon were analyzed. Later the virtual photon $F_2(x, Q^2, P^2)$ was investigated up to NNLO [7] using the results of the three-loop anomalous dimensions for the quark and gluon operators [8] and of the three-loop photon-parton splitting functions [9]. The NNLO result is shown in Fig. 1 together with three curves: the LO,

NLO QCD results and the box (tree) diagram contribution [5],

$$F_2^{\gamma(\text{Box})}(x, Q^2, P^2) = \frac{3\alpha}{\pi} n_f \langle e^4 \rangle \left\{ x \left[x^2 + (1-x)^2 \right] \ln \frac{Q^2}{P^2} - 2x \left[1 - 3x + 3x^2 + (1-2x+2x^2) \ln x \right] \right\},$$

where $n_f \langle e^4 \rangle = \sum_{i=1}^{n_f} e_i^4$ with e_i being the electric charge of the active quark with flavor i and n_f is the number of active quarks. We observe that the NNLO corrections reduce $F_2(x, Q^2, P^2)$ at large x .

Regarding the longitudinal structure function F_L^γ , its LO contribution which is of order α , was calculated in QCD for the real photon ($P^2=0$) target in Ref. [3]. The analysis was made for the case of the virtual photon $F_L^\gamma(x, Q^2, P^2)$ ($\Lambda^2 \ll P^2 \ll Q^2$) in LO [5] and extended up to NLO ($\mathcal{O}(\alpha\alpha_s)$) [7]. The results for the virtual photon target are shown in Fig. 2, where the box (tree) diagram contribution is expressed by $F_L^{\gamma(\text{Box})}(x, Q^2, P^2) = \frac{3\alpha}{\pi} n_f \langle e^4 \rangle \{ 4x^2(1-x) \}$.

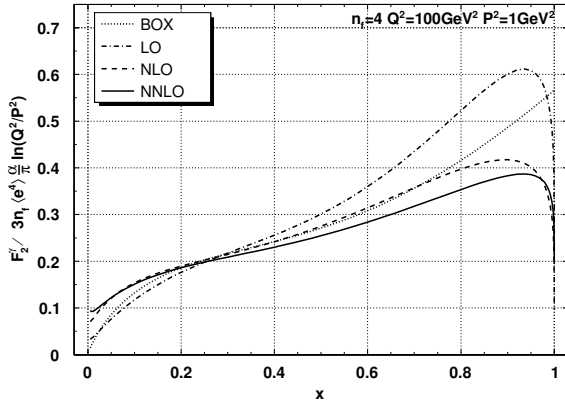


Fig. 1: Virtual photon structure function $F_2^\gamma(x, Q^2, P^2)$ in units of $(3\alpha n_f \langle e^4 \rangle / \pi) \ln(Q^2/P^2)$ for $Q^2 = 100 \text{ GeV}^2$ and $P^2 = 1 \text{ GeV}^2$ with $n_f = 4$ and $\Lambda = 0.2 \text{ GeV}$. [7]

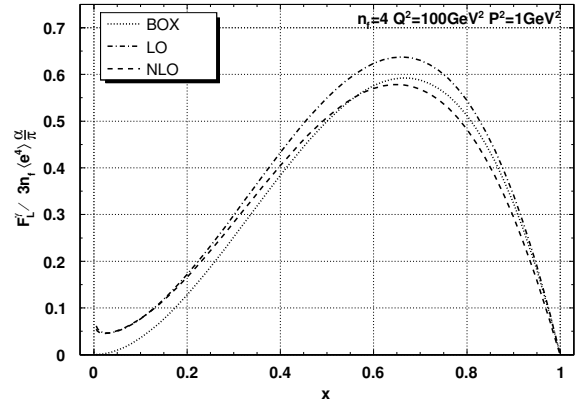


Fig. 2: Longitudinal photon structure function $F_L^\gamma(x, Q^2, P^2)$ in units of $(3\alpha n_f \langle e^4 \rangle / \pi)$ for $Q^2 = 100 \text{ GeV}^2$ and $P^2 = 1 \text{ GeV}^2$ with $n_f = 4$ and $\Lambda = 0.2 \text{ GeV}$. [7]

In the framework of the QCD improved parton model, the structure function F_2^γ is expressed in a factorized form, i.e., as convolutions of coefficient functions and parton distributions in the photon:

$$F_2^\gamma(x, Q^2, P^2) = \sum_i C_2^i \otimes q_i^\gamma + C_2^G \otimes G^\gamma + C_2^\gamma \otimes \Gamma^\gamma \quad (3)$$

where q_i^γ , G^γ and Γ^γ are quark (with i -flavour), gluon and photon distributions, respectively, and C_2^i , C_2^G and C_2^γ are corresponding coefficient functions. In the leading order of α , Γ^γ does not evolve with Q^2 and we set $\Gamma^\gamma = \delta(1-x)$, which means that C_2^γ contributes directly to F_2^γ . These parton distribution functions satisfy the well known DGLAP evolution eqs. Solving the DGLAP eqs. with the appropriate initial conditions at P^2 one obtains the parton distributions at Q^2 . But the coefficient functions and parton distributions are dependent on the factorization-scheme (FS) adopted for defining these quantities. It is the standard choice to use the modified minimal subtraction ($\overline{\text{MS}}$) scheme for the multi-loop calculations of the relevant quantities, namely, the coefficient functions, the splitting functions of partons and the β function parameters. Using these results one obtains the parton distributions in the $\overline{\text{MS}}$ scheme. However it was observed [6, 10] that the multi-loop photonic $\overline{\text{MS}}$ contributions to C_2^γ are negative and singular for $x \rightarrow 1$ and that, in the $\overline{\text{MS}}$ scheme, these singularities have to be compensated by the quark distributions which thus have rather different behaviours at NLO and NNLO from the LO contribution. Under such circumstance a new factorization scheme, which is called DIS_γ , was introduced [10]. In this scheme the photonic coefficient function C_2^γ , which is the direct photon contribution to F_2^γ in $\overline{\text{MS}}$ scheme, is absorbed into the quark distributions, so that $C_2^\gamma|_{\text{DIS}_\gamma} = 0$ while the gluon distribution G_2^γ is intact, i.e., $G_2^\gamma|_{\text{DIS}_\gamma} = G_2^\gamma|_{\overline{\text{MS}}}$.

Parton distributions in the real photon were investigated up to NNLO [6]. For the case of the virtual photon the analyses were made at NLO [11] and NNLO [12]. The results of the flavour-singlet-quark distribution $q_S^\gamma \equiv \sum_i q_i^\gamma$ in the virtual photon are shown in Fig. 3 ($\overline{\text{MS}}$ scheme) and in Fig. 4 (DIS_γ). We observe that (i) the quark distribution shows quite different behaviours in two schemes, especially in large- x region; (ii) in $\overline{\text{MS}}$ scheme, the behaviours of the (LO+NLO) and (LO+NLO+NNLO) curves are quite different from the LO curve. They lie below the LO curve for $0.2 < x < 0.8$ but diverge as $x \rightarrow 1$; (iii) in DIS_γ scheme, the three curves LO, (LO+NLO) and (LO+NLO+NNLO) rather overlap below $x = 0.6$, which means that the NLO and NNLO contributions to the quark distribution are small for moderate x — appropriate behaviours from the viewpoint of “perturbative stability” [6]; (iv) the gluon distribution in the photon is very small in absolute value except in small- x region.

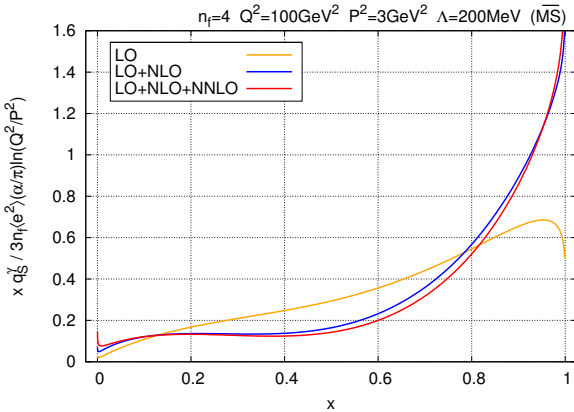


Fig. 3: Singlet-quark distribution $xq_S^\gamma(x, Q^2, P^2)$ in $\overline{\text{MS}}$ scheme. [12]

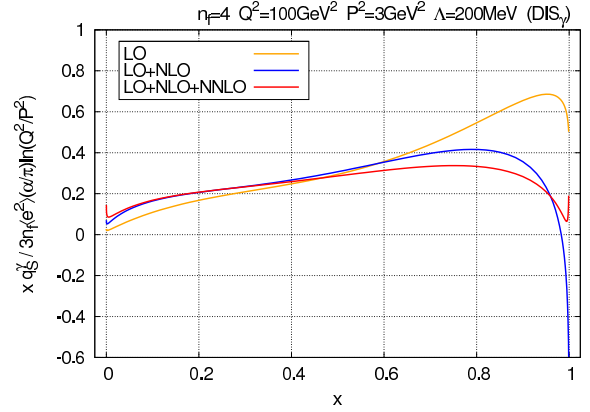


Fig. 4: Singlet-quark distribution $xq_S^\gamma(x, Q^2, P^2)$ in DIS_γ scheme. [12]

A heavy quark h with mass m_h^2 (here, charm and beauty in mind) contributes to the structure function $F_2^\gamma(x, Q^2)$ when $(p+q)^2 = Q^2(\frac{1}{x} - 1) > (2m_h)^2$. There are several approaches in which the heavy-quark mass effects are taken into account. In the fixed flavour-number scheme (FFNS), heavy quarks only appear in the final state of the process and their contributions are described by the heavy-quark coefficient functions [13, 14]. The distributions $q_h(x, Q^2)$ are set to be zero. The FFNS is not appropriate when $Q^2 \gg m_h^2$. In the zero-mass variable flavour-number scheme (ZVFNS), heavy-quark distributions appear similar to the light partons. When Q^2 is larger than a threshold associated with a heavy quark (usually taken as $Q^2 = m_h^2$), this quark is considered as an extra massless parton [15]. The distribution $q_h(x, Q^2)$ differs from zero when $Q^2 > m_h^2$ but otherwise $q_h(x, Q^2) = 0$. The ZVFNS is not appropriate if $Q^2 \approx m_h^2$. The third one is called as the ACOT(χ) scheme [16, 17], which combines both features of the FFNS and ZVFNS. In order to treat the kinematical threshold for the heavy-quark production correctly, it introduces a new variable $\chi_h \equiv x(1 + 4m_h^2/Q^2)$ and modifies the integration range of convolution as follows: $\int_x^1 \frac{dy}{y} f(y) C(\frac{x}{y}) \Rightarrow \int_{\chi_h}^1 \frac{dy}{y} f(y) C(\frac{x}{y})$. Experimental data analyses of F_2^γ with heavy-quark mass effects taken into account have been performed by several groups [13–15, 17, 18]. But we need more data to refine models for the treatment of heavy-quark contributions.

4 Photon structure functions — Future

With the discovery of the Higgs boson at the LHC, plans for building the next-generation e^+e^- colliders [19] are attracting growing attention. In these collider machines, we may obtain highly polarized e^+ and e^- beams. Using these polarized beams we can study another aspect of the photon: its spin structure. For a recent review see [20]. The QCD analysis of the polarized structure function $g_1^\gamma(x, Q^2)$ for a real photon target was performed in LO [21] and in NLO [22, 23]. The polarized virtual photon structure function $g_1^\gamma(x, Q^2, P^2)$ with $\Lambda^2 \ll P^2 \ll Q^2$ was investigated up to NLO in QCD [24]. At $P^2 = 0$, the

structure function g_1^γ satisfies a remarkable sum rule, which is non-perturbative and independent of Q^2 , due to gauge invariance [25, 26]:

$$\int_0^1 g_1^\gamma(x, Q^2) dx = 0. \quad (4)$$

But when the target photon becomes off-shell, $P^2 \neq 0$, the first moment of $g_1^\gamma(x, Q^2, P^2)$ does not vanish any more. The NLO result in QCD for the case $\Lambda^2 \ll P^2 \ll Q^2$ is [24, 26],

$$\int_0^1 dx g_1^\gamma(x, Q^2, P^2) = -\frac{3\alpha}{\pi} \left[\sum_{i=1}^{n_f} e_i^4 \left(1 - \frac{\alpha_s(Q^2)}{\pi} \right) - \frac{2}{\beta_0} \left(\sum_{i=1}^{n_f} e_i^2 \right)^2 \left(\frac{\alpha_s(P^2)}{\pi} - \frac{\alpha_s(Q^2)}{\pi} \right) \right]. \quad (5)$$

The first term in the square brackets resulted from the QED axial anomaly while the second term from the QCD axial anomaly. The sum rule was extended up to NNLO in QCD [27].

5 Epilogue

For future investigation on the photon structure, we still need to understand: (i) hadronic contributions to photon; (ii) heavy-quark mass effects; (iii) transition from real to virtual photon target; (iv) behaviours of F_2^γ and parton distributions near $x = 0$ and $x = 1$; (v) the spin structure of photon. To that end it is essential for us to have more new experimental data on the photon structure.

Acknowledgements

We wish to thank the organizers of Photon 2017 for the hospitality at such a stimulating conference.

References

- [1] T.F. Walsh, *Phys. Lett. B* **36** (1971) 121; S.J. Brodsky, T. Kinoshita and H. Terazawa, *Phys. Rev. Lett.* **27** (1971) 280.
- [2] T.F. Walsh and P.M. Zerwas, *Phys. Lett. B* **44** (1973) 195; R.L. Kingsley, *Nucl. Phys.* **60** (1973) 45.
- [3] E. Witten, *Nucl. Phys. B* **120** (1977) 189.
- [4] W.A. Bardeen and A.J. Buras, *Phys. Rev. D* **20** (1979) 166; *Phys. Rev. D* **21** (1980) 2041(E).
- [5] T. Uematsu and T. F. Walsh, *Phys. Lett. B* **101** (1981) 263 ; *Nucl. Phys. B* **199** (1982) 93.
- [6] S. Moch, J.A.M. Vermaseren and A. Vogt, *Nucl. Phys. B* **621** (2002) 413.
- [7] T. Ueda, K. Sasaki and T. Uematsu, *Phys. Rev. D* **75** (2007) 114009.
- [8] S. Moch, J.A.M. Vermaseren and A. Vogt, *Nucl. Phys. B* **688** (2004) 101; **691** (2004) 129.
- [9] A. Vogt, S. Moch and J.A.M. Vermaseren *Acta. Phys. Pol. B* **37** (2006) 683; arXiv:hep-ph/0511112.
- [10] M. Glück, E. Reya and A. Vogt, *Phys. Rev. D* **45** (1992) 2749.
- [11] M. Glück, E. Reya and M. Stratmann, *Phys. Rev. D* **51** (1995) 3220.
- [12] T. Ueda, K. Sasaki and T. Uematsu, *Eur. Phys. J. C* **62** (2009) 467.
- [13] M. Glück, E. Reya and A. Vogt, *Phys. Rev. D* **46** (1992) 1973; M. Glück, E. Reya and I. Schienbein, *Phys. Rev.* **60** (1999) 054019; **62** (2000) 019902(E).
- [14] E. Laenen, S. Riemersma, J. Smith and W.L. van Neerven, *Phys. Rev. D* **49** (1994) 5753.
- [15] P. Aurenche, M. Fontannaz, J.Ph. Guillet, *Z. Phys. C* **64** (1994) 621 ; *Eur. Phys. J. C* **44** (2005) 395.
- [16] S. Kretzer, C. Schmidt and W.K. Tung, *J. Phys. G* **28** (2002) 983; S. Kretzer, H.L. Lai, F.I. Olness and W.K. Tung, *Phys. Rev. D* **69** (2004) 114005.
- [17] F. Cornet, P. Jankowski, M. Krawczyk and A. Lorca, *Phys. Rev. D* **68** (2003) 014010; F. Cornet, P. Jankowski and M. Krawczyk, *Phys. Rev. D* **70** (2004) 093004.
- [18] W. Słominski, H. Abramowicz and A. Levy , *Eur. Phys. J. C* **45** (2006) 633.

- [19] <http://www.linearcollider.org>; <http://tlep.web.cern.ch>; <http://cepc.ihep.ac.cn>.
- [20] G. M. Shore, *Eur. Phys. J. C* **73** (2013) 2340.
- [21] K. Sasaki, *Phys. Rev. D* **22** (1980) 2143; *Prog. Theor. Phys. Suppl.* **77** (1983) 197.
- [22] M. Stratmann and W. Vogelsang, *Phys. Lett. B* **386** (1996)370.
- [23] M. Glück, E. Reya and C. Sieg, *Phys. Lett. B* **503** (2001) 285; *Eur. Phys. J. C* **20** (2001) 271.
- [24] K. Sasaki and T. Uematsu, *Phys. Rev. D* **59** (1999) 114011; T. Ueda, K. Sasaki and T. Uematsu, *Phys. Lett. B* **640** (2006) 188.
- [25] S. D. Bass, *Int. J. Mod. Phys. A* **7** (1992) 6039; A. Freund and L. M. Sehgal, *Phys. Lett. B* **341** (1994) 90; S. D. Bass, S. J. Brodsky and I. Schmidt, *Phys. Lett. B* **437** (1998) 424.
- [26] S. Narison, G. M. Shore and G. Veneziano, *Nucl. Phys. B* **391** (1993) 69.
- [27] K. Sasaki, T. Ueda and T. Uematsu, *Phys. Rev. D* **73** (2006) 094024.